JOURNAL OF SOLID STATE CHEMISTRY 82, 216–224 (1989)

Anharmonic Thermal Motion of Ag in $AgCrSe_2$: A High-Temperature Single-Crystal X-Ray Diffraction Study

A. VAN DER LEE AND G. A. WIEGERS

Laboratory of Inorganic Chemistry, Materials Science Center of the University, Nijenborgh 16, 9747 AG Groningen, The Netherlands

Received March 16, 1989

The thermal motion of Ag in the two-dimensional silver ion conductor $AgCrSe_2$ (at 295 K; a = 3.6798(2) Å, c = 21.225(2) Å; Z = 3; spacegroup $R3m$) is studied as a function of temperature by single-crystal X-ray diffraction. At room temperature the Ag atoms occupy only one-half of the available tetrahedral holes between the $CrSe_2$ sandwiches. Disordering of the silver sublattice over all tetrahedral sites proceeds second order with T_c = 475 K: above T_c the spacegroup is $R\bar{3}m$. Refinements were performed with data measured at six different temperatures in the range 295–673 K. Anharmonic temperature factors of Ag based on the Gram–Charlier expansion have been refined up to fourth order. R_w values range from 0.022 to 0.049, the number of variables from 17 to 22. The refinements confirm the second-order nature of the order–disorder transition. Below T_c the largest thermal vibrations are directed to the octahedral sites between the $CrSe_2$ sandwiches. The plane between the α- and β-lattice plays a crucial role. The joint probability density function (jpdf) of Ag is high in regions surrounding the projected α- and β-sites and the octahedral site; at these sites the jpdf shows a minimum. The diffusion of Ag from an α- to a β-site proceeds therefore via this intermediate plane.

Introduction

The isostructural compounds $MCrX_2$ (M = Cu, Ag and X = S, Se) are known to be excellent M-ion conductors, owing to quasi-two-dimensional diffusion of M-ions (*1–4*). All these compounds undergo a second-order phase transition at which the silver (copper) sublattice becomes disordered. The structures of these rhombohedral compounds (in hexagonal description a = 3.4–3.7 Å, c = 18–22 Å; spacegroup $R3m$; Z = 3; Fig. 1a) are based on a distorted cubic close-packing of the anions. Sandwiches CrX_2^- are present with Cr^{3+} cations in octahedral coordination by X^{2-} anions. The tetrahedral sites between the sandwiches CrX_2^- form a slightly puckered honeycomb lattice, consisting of two interpenetrating triangular lattices denoted by α and β (Fig. 1b). It may be noted that there is a small difference in z-coordinate between an α-site and a β-site. For that reason the distribution of silver or copper is called quasi-two-dimensional. Neighboring "planes" of silver (copper) are $c/3 \approx 7$ Å apart. Well below the phase transition one sublattice (say the α-lattice) is fully occupied by Ag (Cu). At higher temperatures a gradual disordering takes place over the two sublattices α and β, the disordering being complete at T_c = 475 K for $AgCrSe_2$ (*3*). At T_c the spacegroup symmetry changes from $R3m$ to the centrosymmetric spacegroup $R\bar{3}m$.

Previous single-crystal X-ray diffraction

0022-4596/89 $3.00

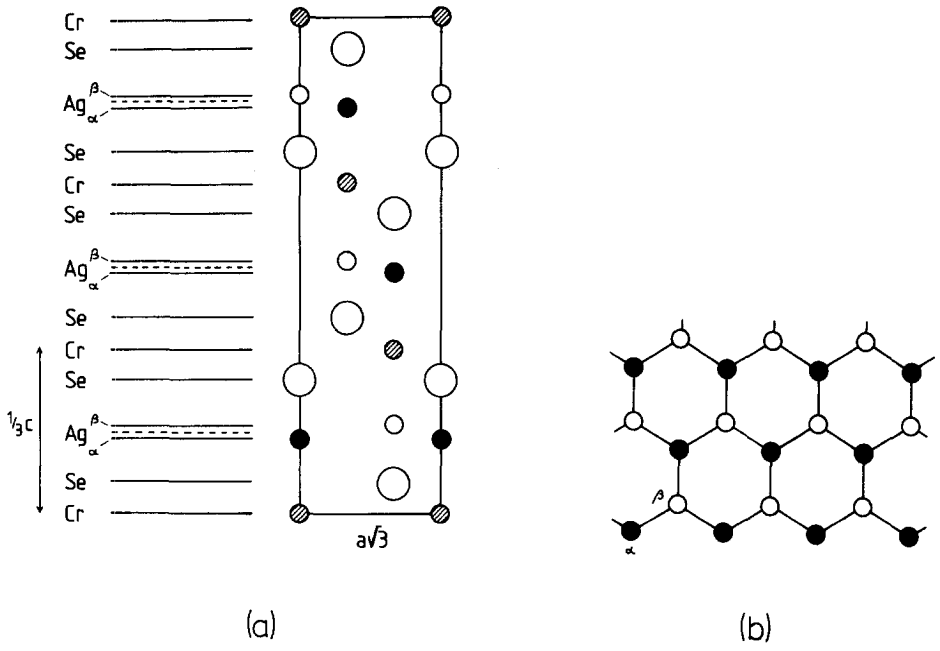

FIG. 1. (a) $(11\bar{2}0)$ Section of the structure of $MCrX_2$; large open circles are X, small hatched circles are Cr, small open circles are M at α; the β-sites are indicated by small closed circles. (b) The puckered honeycomb lattice formed by α- and β-sites.

investigation on $AgCrS_2$ showed that at room temperature the amplitude of thermal motion of Ag in the *ab*-plane is approximately three times larger than that along the *c*-axis (*3*). A difference Fourier synthesis showed residual densities around the silver sites pointing to an anharmonicity in the thermal motion. In the harmonic approximation anisotropic thermal motion is described by U_{11} parallel (001) and U_{33} along [001]. The anharmonicity is determined by the site symmetry $3m$ of Ag, putting restrictions on the number of the higher order tensor elements (see below).

In this paper we study the behavior of the anharmonic thermal motion of Ag in $AgCrSe_2$ as a function of temperature by means of single-crystal X-ray diffraction. We apply the Gram–Charlier expansion of the probability density function and its corresponding Fourier transform, i.e., the temperature factor, to account for anharmonic motion. The disordering of the silver sublattice below the phase transition, as well as the disordered sublattice above T_c, will be discussed on the basis of single and joint probability density functions.

Experimental

$AgCrSe_2$ powder was obtained by synthesis from the elements. Single crystals of $AgCrSe_2$ grow in 5 days by vapor transport in a temperature gradient 870–760°C, using bromine as the transport agent. The crystals used for X-ray data collection are platelets and have dimensions of typically 0.25 × 0.25 × 0.04 mm^3. Test measurements were carried out to select suitable crystals. The crystal was mounted upon a quartz fiber with Torr Seal vacuum sealing kit. This fiber was inserted in a 0.3-mm-diameter quartz capillary to prevent oxidation at high temperatures.

The intensities of the reflections were measured on a CAD-4H kappa diffractometer (Enraf-Nonius), equipped with a special furnace as described by Tuinstra and Fraase Storm (5). The ω-2θ scan method was applied with a ω-scan angle of $(0.95 + 0.35 \tan\theta)°$. Mo$K\alpha$ radiation and a graphite monochromator were used.

Data collection was carried out at six different temperatures between 295 and 673 K. Two crystals of the same batch were used for the structure investigations. The crystal had to be replaced after the first four datasets because of the accidental cracking of the quartz capillary. As will be shown later, this had little consequences on the results. At each temperature about 1900 reflections with $-7 \le h \le 7$, $0 \le k \le 7$, $-45 \le l \le 45$ were measured with the conditions: $\sin\theta/\lambda \le 1.077$ Å and $-h + k + l = 3n$, the rhombohedral reflection condition. The intensities were corrected for Lorentz polarization and absorption ($\mu = 324$ cm^{-1}) (6). After averaging over equivalent reflections, the intensities of 375 reflections were available for structure refinements. Reflections with $|F_{obs}| < 2.5\ \sigma(|F_{obs}|)$ were not used in the refinements. The total number of these reflections increased from only 1 at 295 K up to 25 at 673 K.

Refinement of the Structure

All structure refinements and calculations were carried out with the program system **PROMETHEUS** (7). Anharmonic temperature factors based on the Gram–Charlier formalism were used,

$$T(h_1, h_2, h_3) = T_{harm}(h_1, h_2, h_3) \left[1 + \frac{(2\pi i)^3}{3!} \sum\sum\sum C_{pqr} h_p h_q h_r + \frac{(2\pi i)^4}{4!} \sum\sum\sum\sum D_{pqrs} h_p h_q h_r h_s + \cdots\right], \quad (1)$$

where h_1, h_2, and h_3 are the Miller indices; C_{pqr} and D_{pqrs} are the third- and fourth-order tensor elements respectively; and $i = \sqrt{-1}$. The occurrence of i in the temperature factor reflects the possibility of a noncentrosymmetric probability density function.

The use of this expansion and other expansions to describe anharmonic thermal motion has been extensively discussed by Zucker and Schulz (8, 9). The anharmonic temperature factor was used only for silver, since the other atoms did not show deviations from the harmonic description. The point symmetry of the Ag-site ($3m$) requires two independent second-order, three third-order, four fourth-order, five fifth-order, and seven sixth-order thermal motion tensor elements (10, 11). The occupancy of the available silver sites was constrained by the condition $p_\alpha + p_\beta = 1$ for refinements at $T < T_c$. Furthermore, the thermal parameters of Ag-ions at α- and β-sites were kept equal.

Atomic scattering factors and correction terms for anomalous dispersion were taken from *International Tables for X-ray Crystallography* (10).

To fix the origin in the noncentrosymmetric low-temperature phase Cr was kept fixed at (0, 0, 0). The absolute configuration of the crystal, i.e., the occupancy of α and β at room temperature, was determined by a refinement with reflections transformed from (hkl) to $(\bar{h}\bar{k}\bar{l})$. The refinement with the lower R-factor was regarded as belonging to the correct configuration.

The atomic parameters, one scale-factor, and one isotropic extinction parameter were refined. The function minimized was $\sum w(|F_{obs}| - |F_{cal}|)^2 / \sum w|F_{obs}|^2$, with $w = 1/\sigma^2$.

As starting values for the atomic parameters at 295 K, the values of Engelsman *et al.* (12) were used, as obtained by neutron powder diffraction.

Anharmonic Thermal Motion of Ag in $AgCrSe_2$

The Low-Temperature Phase

The coordinates and temperature factors resulting from the harmonic refinements at

TABLE I

RESULTS OF THE REFINEMENT WITH HARMONIC TEMPERATURE FACTORS AT $T = 295$ K

	Ag	Cr	Se(1)	Se(2)
p	1.0000	1.0000	1.0000	1.0000
z	0.1520(2)	0.0000	0.2692(1)	0.7328(1)
U_{11}	0.0826(9)	0.0079(3)	0.0080(5)	0.0080(5)
U_{33}	0.0113(4)	0.0082(5)	0.0069(4)	0.0103(4)

Note. (a) Spacegroup $R3m$ with hexagonal axes (obverse setting): $a = 3.6798(2)$ Å, $c = 21.225(2)$ Å. (b) Standard deviations in the last decimal are given in parentheses. (c) p = occupancy of the site; $z = z$ coordinate. (d) The harmonic temperature factor is of the form $\exp(-T)$, where $T = 2\pi^2 \sum h_i h_j U_{ij} a_i^* a_j^*$.

room temperature (Table I) agree nicely with those reported by Engelsman *et al.* (*12*).

The mean-square displacement in the *ab*-plane ($U_{11} = 0.0826$ Å^2) is of the same magnitude as the largest mean-square displacements in well-known solid electrolytes in their low-temperature phase at room temperature. For example, Yoshiasa *et al.* (*13*) report 0.08 Å^2 for Ag in AgI; Schulz *et al.* (*14*) give 0.01 Å^2 for Pb and 0.02 Å^2 for F in PbF_2. More striking however is the very large ratio U_{11}/U_{33}, displaying the two-dimensional character of the ionic diffusion.

In Table II the positional and thermal parameters for Ag at the six temperatures of measurements are given. Since we focus on the thermal motion of Ag, we here omit all the refined parameters of the other atoms. Coordinates and thermal parameters of all atoms and $|F_{obs}|$, $|F_{cal}|$, $\sigma(|F_{obs}|)$ for the six temperatures of data collection are given in separate tables.[1]

[1] See NAPS Document No. 04716 for 19 pages of supplementary materials from ASIS/NAPS, Microfiche Publications, P.O. Box 3513, Grand Central Station, New York, New York 10163. Remit in advance $4.00 for microfiche copy or for photocopy, $7.75 up to 20 pages plus $.30 for each additional page. All orders must be prepared.

The decrease of the reliability factor R_w when adding anharmonic tensor elements to the harmonic temperature factor proves the presence of anharmonicity in the thermal motion of silver. A check on the physical significance of the higher order tensor elements was performed by calculating the Fourier transform of the temperature factor, i.e., the probability density function (pdf) of the atom. It is known that none of the anharmonic temperature factors, which are in use for general site symmetries, exclude that their corresponding pdf's are nonnegative everywhere for all values of the parameters (*15*). Therefore, to make physical sense, the pdf should not have deep negative regions in central parts.

Only third- and fourth-order tensor elements were used in the refinements. Adding fifth-order tensor elements either improved the model very little ($T = 295$ K), or gave physical meaningless pdf's. In all pdf's some small negative regions were calculated: the ratio |min(pdf)|/max(pdf) was mostly less than 0.05; only the 475 K refinement gave a larger ratio of 0.15. The small negative regions can be found in the tails of the distributions.

The pdf maps of the planes $z = z(Ag_\alpha)$ for 295, 400, and 450 K are shown in Fig. 2. The largest amplitudes are toward the octahedral sites. This means that a silver ion at an α-site does not jump through the edge of the tetrahedron (the direct way), but instead follows an indirect way through the faces of the tetrahedron to reach the β-site. By using inelastic neutron scattering, infrared spectroscopy, and model calculations, Brüesch *et al.* (*16*) arrived at the same conclusion in the case of $AgCrS_2$.

Just below the phase transition (Fig. 2c) the pdf map displays some splitting in the central region. The distance of the modes (i.e., the local maxima in the pdf) to the central site is about 0.6 Å. This distribution does not imply that there is a static distribution at these three off-center sites. Limita-

TABLE II

RESULTS OF THE REFINEMENTS FOR Ag

T (K)	295	400	450	500	573	673
Spgr	$R3m$	$R3m$	$R3m$	$R\bar{3}m$	$R\bar{3}m$	$R\bar{3}m$
p	1.0000	0.855(6)	0.646(9)	0.5000	0.5000	0.5000
z	0.1531(2)	0.1558(3)	0.1579(5)	0.1561(3)	0.1567(4)	0.1590(9)
U_{11}	0.094(2)	0.188(5)	0.25(1)	0.271(5)	0.297(6)	0.34(1)
U_{33}	0.017(1)	0.025(1)	0.028(2)	0.035(2)	0.039(2)	0.054(4)
C_{111}	−0.22(3)	−1.1(1)	−2.8(4)	−2.0(1)	−2.3(1)	−3.4(2)
C_{333}	0.00011(3)	0.00018(7)	0.0003(1)	0.0003(1)	0.0005(1)	0.0011(3)
C_{113}	0.021(2)	0.12(7)	0.26(2)	0.20(1)	0.22(1)	0.31(3)
D_{1111}	0.47(8)	2.8(5)	3(1)	2.7(7)	3.4(8)	3(2)
D_{3333}	0.000035(8)	0.00002(1)	0.00001(2)	0.00004(1)	0.00005(2)	0.00007(6)
D_{1113}	−0.002(2)	0.017(9)	0.14(4)	0.02(2)	0.03(3)	0.18(9)
D_{1133}	0.0008(2)	−0.017(8)	−0.023(3)	−0.006(1)	−0.007(2)	−0.022(6)
N	375	374	372	368	355	351
$R_w(1)$	0.034	0.053	0.061	0.073	0.068	0.087
$R_w(2)$	0.022	0.028	0.040	0.033	0.028	0.049

Note. (a) p = Occupancy of the α-site; z = z coordinate of Ag; N = number of reflections with $|F_{obs}| < 2.5\sigma(|F_{obs}|)$.

$$\text{(b)}\quad R_w = \left[\frac{\sum (w(|F_{obs}| - |F_{cal}|)^2)}{\sum (w|F_{obs}|^2)}\right]^{1/2}, \quad w = 1/\sigma^2.$$

(c) $R_w(1)$ is the agreement factor after refinements with only harmonic temperature factors; $R_w(2)$ results after including tensor elements up to the fourth order. Third- and fourth-order tensor elements C_{pqr} and D_{pqrs} have been multiplied by, respectively, 10^3 and 10^4.

tions, strengths, and examples of different methods to describe multimodal atomic probability densities have been discussed by Kuhs (*17*).

The disordering of the α-sublattice is demonstrated very well with the simultaneous refinement of the occupation probability of the α- and the β-sites (p_α and p_β). At room temperature the α-sublattice is fully occupied. A refinement of the occupation of the β-site gives a nonsignificant occupation. At 400 K the refinements yield the best results with $p_\alpha = 0.85$. In the last 50 K below the phase transition the disordering goes very fast, as predicted by theoretical models for this order–disorder transition (*3, 18, 19*). In order to compare the long-range order parameter ($L(T) = 2p_\alpha(T) - 1$) of the order–disorder transition with L for the theoretical models, the occupation probability should be determined for a range of temperatures. It is our opinion not to draw definite conclusions on the temperature dependence of the long-range order parameter from the temperature dependence of the intensity of some silver sensitive reflections (e.g., 104, 015) as was done by Yakshibayev *et al.* (*4*) for $CuCrSe_2$. These authors found a transition temperature (no change in intensity) about 120 K below T_c known from DTA and ionic conductivity measurements. The authors ascribe the discrepancy to experimental conditions (high background level). In our case we found a similar behavior, which shows that such intensity measurements result in a misleading interpretation of the transition. The only way to compare experimental and theoretical models is by refinements on full data sets.

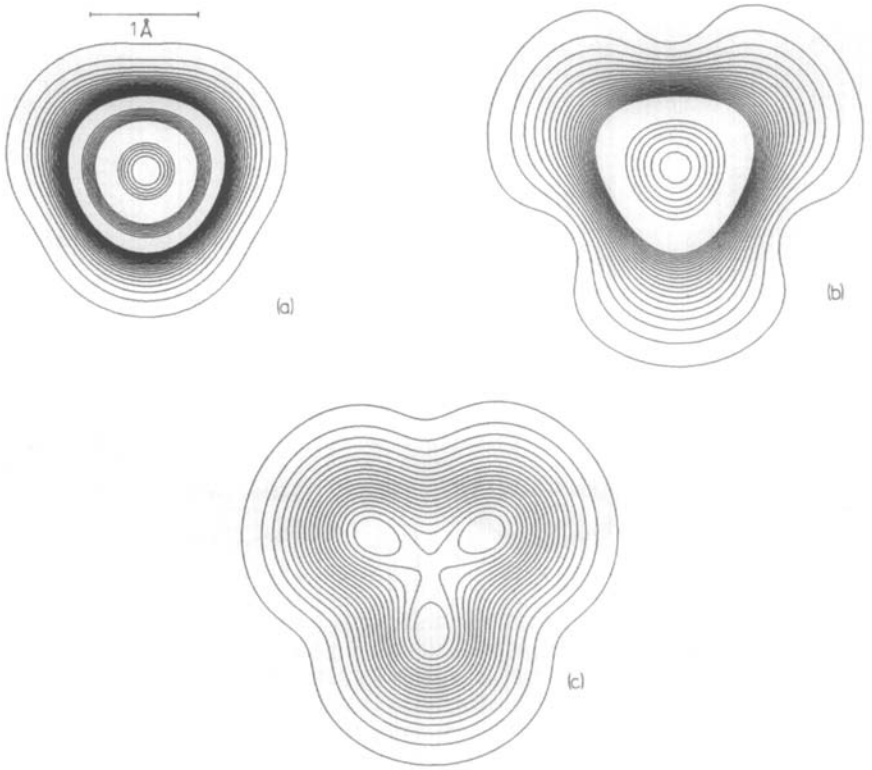

FIG. 2. Single pdf's of Ag in the plane parallel (001) at $z = z(Ag_\alpha)$. (a) $T = 295$ K; (b) $T = 400$ K; (c) $T = 450$ K. Contourlines 6, 16, 26, . . . , 186; 400, 450, . . . , 700; 1500, 1600, . . . , 1900 $Å^{-3}$. The lobes are directed to the octahedral sites.

The High-Temperature Phase

The high-temperature phase of $AgCrSe_2$ can be regarded as a superionic phase; the ionic conductivity just above the phase transition is about 20 SM^{-1} (*2*). The ionic conductivity however does not show the usual type of Arrhenius behavior because of the order–disorder transition (*1, 3, 18*). Results of the refinements can also be found in Table II. The decrease of the reliability factor R_w when going from 500 to 573 K is probably due to a better absorption correction for the second crystal used for measurements at 573 and 673 K. When we compare the results of refinements at 500 K (first crystal) and 573 and 673 K (second crystal) there are no anomalous jumps in the parameters. So we assume that the use of a second crystal does not affect the interpretation of the results.

In the superionic phase the amplitudes of thermal vibration become comparable with interionic distances. In the overlap region the value of the pdf cannot be uniquely determined. Instead the joint probability distribution function (jpdf) has to be used (*20*). The jpdf is defined by the equation

$$\text{jpdf}(\mathbf{r}) = \sum_i p_i[\text{pdf}_i(\mathbf{r})] \qquad (2)$$

with p_i the occupancy of site i, the summation being taken over all occupied sites. The probability of finding the atom in a small volume element $d\mathbf{r}$ around $\mathbf{r}$ is given jpdf($\mathbf{r}$) multiplied with $d\mathbf{r}$. By calculating

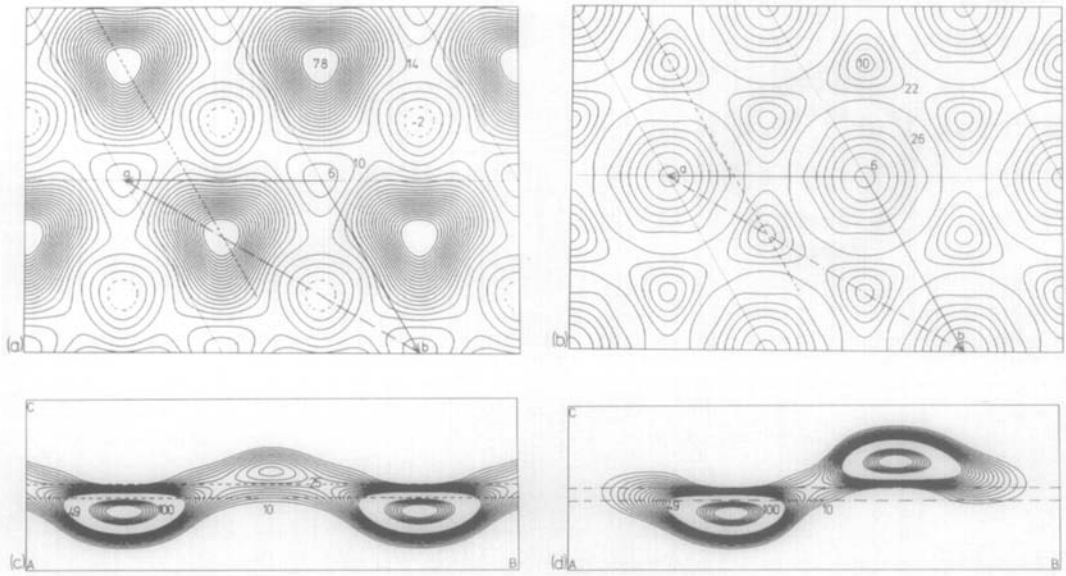

FIG. 3. Joint pdf of Ag at $T = 673$ K. (a) Plane parallel (001) at $z = z\,(ag_\alpha)$; the β- and octahedral sites projected at $(\frac{1}{3}, \frac{2}{3})$ and the origin, respectively. (b) Plane parallel (001) halfway to the α- and β-sublattice, the octahedral sites at the origin. (c) The plane parallel [001] defined by $A = (\frac{2}{3}, -1, 0.45)$, $B = (\frac{2}{3}, \frac{2}{3}, 0.45)$, and $C = (\frac{2}{3}, -1, 0.55)$. (d) The plane parallel c defined by $A = (1, 0, 0.45)$, $B = (0, 1, 0.45)$, and $C = (1, 0, 0.55)$. The planes in (c) and (d) are perpendicular to the planes in (a) and (b). Hatched straight lines in (a) and (b) correspond with those in (c) and (d). Contourlines (a) and (b): $-2, 2, \ldots,$ 78 Å^{-3}; (c) and (d): 10, 13, . . . , 49; 100, 106, . . . , 130 Å^{-3}.

the jpdf in appropriate sections, one can trace the possible diffusion paths.

In the case of $AgCrSe_2$ the need to use the jpdf in the high-temperature phase becomes clear by comparing maps calculated with single pdf's and with a jpdf. The single pdf's show roughly the same features as those below the phase transition, i.e., three lobes toward the octahedral sites, but they become increasingly flat. Thus a significant overlap of two neighboring pdf's has to be expected. In Fig. 3 the jpdf of the Ag-atom at 673 K in four different sections is shown. The jpdf's of 500 and 573 K resemble the jpdf at 673 K very much, so we confine ourselves to that temperature.

The jpdf shows features which cannot be resolved by single pdf's. Figure 3a shows a section parallel (001) through the α-sublattice. The largest thermal vibrations are no longer directed to the octahedral sites. A saddle point is present halfway to α–α sites (and β–β sites) in two neighboring unit cells. This corresponds to a diffusion between silver sites in the α-sublattice. The same applies to the β-sublattice. A more probable diffusion path however can be detected by inspecting the sections given in Figs. 3b–3d. In the plane with the z-coordinate of the octahedral site (Fig. 3b), we find large values of the jpdf (compared with the value at the mode) in bands surrounding the octahedral sites; a minimum density is found at the octahedral sites and at the projected α- and β-sites. This particular density distribution is due to an overlap of the pdf's of an α-site and a β-site. The sections given in Figs. 3c and 3d are perpendicular to those in Figs. 3a and 3b; to facilitate the recognition of the relative orientation of the

planes, corresponding lines have been indicated by straight hatched lines. By comparing Fig. 3a with Fig. 3c it is clear that the more favorable diffusion path from α to β and from α to α (β to β) is via the plane between the α- and β-sublattice, the sites at the trigonal axes including the octahedral site being avoided. A comparison of Figs. 3c and 3d shows that direct jumps through the edge of the tetrahedron are possible, but they are less likely than the path via the band around the octahedral site. Hibma (*1*) already suggested that off-center octahedral sites, i.e., sites displaced from the true octahedral site, play an important role in the conduction mechanism. The refinement of the occupancy of an octahedral site however need not be necessary when using anharmonic temperature factors. In the case of $AgCrSe_2$ the refinement of the occupancy of the octahedral site resulted in a occupancy of only 0.04 with the same *R*-value, but mostly larger standard deviations. This can hardly be regarded as significant in view of the high point symmetry of the octahedral site ($\bar{3}m$). We conclude therefore that anharmonic temperature factors alone are good enough to describe the silver distribution in the crystal.

Careful inspection of the three-dimensional jpdf shows that the point of maximum probability density—the mode—is somewhat displaced along the trigonal axis with respect to the refined *z*-coordinate (about 0.16 Å). The displacement is directed toward the face of the tetrahedron. This is a common feature of anharmonic probability density functions: the mean of the pdf, i.e., the refined position, need not coincide with the maximum of the pdf.

The probability density function is directly related to the one-particle potential by the formula

$$V(\mathbf{r}) = -kT \ln[\mathrm{pdf}(\mathbf{r})/\mathrm{pdf}(\mathbf{r} = \mathbf{r}_0)], \quad (3)$$

where k is Boltzmann's constant and T is temperature. From this formula one can calculate in principle the activation energy for ionic conductivity. When using the jpdf instead of the pdf in Eq. (3), the results must be carefully interpreted, because it can be shown that in the case of disordered structures a pseudo-potential is obtained, which is strongly temperature dependent (*20*). The lowest barriers in $AgCrSe_2$ (in the plane between the α- and the β-sublattice, see Fig. 3b) obtained with Eq. (3) vary from 0.14(3) eV at 500 K to 0.11(3) eV at 673 K. These values have to be compared with conductivity measurements by Gerards (*3*), who obtained with *ac*-response techniques 0.17(3) eV. The discrepancy may be due to the use of pressed powders in the *ac*-response techniques. On the other hand the presence of static disorder results in an underestimation and a temperature dependency of the activation energy obtained with Eq. (3). The occurrence of the band of maximum density around the octahedral site together with the temperature dependency of the activation energy seems an indication of some static disorder in $AgCrSe_2$.

Acknowledgments

The authors thank Miss R. J. Haange for growing the crystals, and Dr. J. L. de Boer and Mr. J. Spoelstra for help during the single-crystal X-ray measurements.

References

1. T. Hibma, *Solid State Commun.* **33,** 445 (1980).
2. B. A. Boukamp and G. A. Wiegers, *Solid State Ionics* **9–10,** 1193 (1983).
3. A. G. Gerards, Thesis, Groningen, The Netherlands (1987).
4. R. A. Yakshibayev, V. N. Zabolotsky, and R. F. Almukhametov, *Solid State Ionics* **31,** 1 (1988).
5. F. Tuinstra and G. M. Fraase Storm, *J. Appl. Crystallogr.* **11,** 257 (1978).
6. A. L. Spek, "Proceedings of the 8th European Cryst. Meeting, Liege, Belgium (1983)."
7. U. H. Zucker, E. Perenthaler, W. F. Kuhs, R. Bachmann, and H. Schulz, *J. Appl. Crystallogr.* **16,** 358 (1983).

8. U. H. ZUCKER AND H. SCHULZ, *Acta Crystallogr. Sect. A* **38,** 563 (1982).
9. U. H. ZUCKER AND H. SCHULZ, *Acta Crystallogr. Sect. A* **38,** 568 (1982).
10. International Tables for X-ray Crystallography, Vol. IV, Kynoch, Birmingham (1974).
11. W. F. KUHS, *Acta Crystallogr. Sect. A* **40,** 133 (1983).
12. F. M. R. ENGELSMAN, G. A. WIEGERS, F. JELLINEK, AND B. VAN LAAR, *J. Solid State Chem.* **6,** 574 (1973).
13. A. YOSHIASA, K. KOTO, F. KANAMARU, S. EMURA, AND H. HORIUCHI, *Acta Crystallogr. Sect. B* **43,** 434 (1987).
14. H. SCHULZ, E. PERENTHALER, AND U. H. ZUCKER, *Acta Crystallogr. Sect. A* **38,** 729 (1982).
15. C. SCHERINGER, *Acta Crystallogr. Sect. A* **44,** 343 (1988).
16. P. BRÜESCH, T. HIBMA, AND W. BÜHRER, *Phys. Rev. B* **27,** 5052 (1983).
17. W. F. KUHS, *Acta Crystallogr. Sect. A* **39,** 148 (1983).
18. N. L. SHARMA AND T. TANAKA, *Phys. Rev. B* **28,** 2146 (1983).
19. A. G. GERARDS, B. A. BOUKAMP, AND G. A. WIEGERS, *Solid State Ionics* **9–10,** 471 (1983).
20. R. BACHMANN AND H. SCHULZ, *Acta Crystallogr. Sect. A* **40,** 668 (1984).